

High-Speed and Low-Noise SACM Avalanche Photodiodes With an Impact-Ionization-Engineered Multiplication Region

Ning Duan, Shuling Wang, Feng Ma, Ning Li, Joe C. Campbell, Chad Wang, and Larry A. Coldren

Abstract—A separate absorption, charge, and multiplication $\text{In}_{0.53}\text{Ga}_{0.47}\text{As}$ – $\text{In}_{0.52}\text{Al}_{0.48}\text{As}$ avalanche photodiode with an impact-ionization-engineered multiplication region is reported. By implementing an electric field gradient in the multiplication region, better control of impact-ionization can be achieved. Gain-bandwidth product of 160 GHz and excess noise factor with an equivalent k value of 0.1 are demonstrated.

Index Terms—Avalanche photodiodes (APDs), impact ionization, photodetectors.

I. INTRODUCTION

THE separate absorption, charge, and multiplication (SACM) structure avalanche photodiode (APD), which consists of an absorbing region and a multiplication region separated by a charge layer, has been widely studied for high-bit-rate long-haul wide-band optical communication applications. The SACM APD structure has the advantage that the photon absorption process and the impact ionization multiplication process are independent from each other and can be optimized individually to improve both the noise and speed performance. Further, this structure effectively suppresses tunneling in the narrow bandgap-absorbing layer.

Much of the research on these APDs has focused on achieving lower noise and higher gain-bandwidth products to accommodate the ever-increasing bit rates of fiber-optic systems. Lower noise is usually associated with higher speed, since in the gain distributions, the high-gain tail contributes to both higher noise and longer transit time [1]. Very low noise has been achieved in the GaAs–AlGaAs material system by impact ionization engineering (I^2E) [2], [3]. It is now understood that the role of heterojunctions in lowering the multiplication noise of APDs is to spatially localize impact ionization events even with $\alpha/\beta \sim 1$ [4]. To apply the I^2E concept first demonstrated with AlGaAs–GaAs APDs to more practical “long wavelength” materials that are widely used for fiber-optic components, APDs with I^2E multiplication region using AlInGaAs–InAlAs have been reported for a PIN-type structure [5]. However, incorporation of an I^2E multiplication region into an SACM structure with an InGaAs absorber has not been reported. In this letter, we present the design and successful implementation of an SACM



Fig. 1. Schematic layer structure of the SACM APD.

APD with an $\text{In}_{0.52}\text{Al}_{0.48}\text{As}$ – $\text{In}_{0.53}\text{Ga}_{0.17}\text{Al}_{0.3}\text{As}$ I^2E multiplication region.

II. DEVICE STRUCTURE

The structure was grown in a molecular beam epitaxy reactor, on a semi-insulating InP substrate. As shown in Fig. 1, the first layer grown was a 100-nm-thick unintentionally doped $\text{In}_{0.52}\text{Al}_{0.48}\text{As}$ layer to suppress silicon diffusion into the semi-insulating InP substrate from the $\text{In}_{0.52}\text{Al}_{0.48}\text{As}$ n-contact layer, which can cause excessive parasitic capacitance between contact pads. A 500-nm-thick heavily doped n^+ -type (silicon, $\geq 8 \times 10^{18} \text{ cm}^{-3}$) $\text{In}_{0.52}\text{Al}_{0.48}\text{As}$ layer was grown as a buffer layer and was followed by a 500-nm n^+ -type (silicon, $\geq 5 \times 10^{18} \text{ cm}^{-3}$) $\text{In}_{0.52}\text{Al}_{0.48}\text{As}$ contact layer. Following the n-type contact layer was the I^2E multiplication region. The compound multiplication region consisted of an unintentionally doped layer of $\text{In}_{0.52}\text{Al}_{0.48}\text{As}$ with a thickness of 80 nm, an unintentionally doped $\text{In}_{0.53}\text{Ga}_{0.17}\text{Al}_{0.3}\text{As}$ layer with a thickness of 80 nm, a p-type (Be, $2.2 \times 10^{17} \text{ cm}^{-3}$)

Manuscript received April 5, 2005; revised April 26, 2005.

N. Duan, S. Wang, F. Ma, N. Li, and J. C. Campbell are with the University of Texas, Austin, TX 78712 USA (e-mail: jcc@mail.utexas.edu).

C. Wang and L. A. Coldren are with the University of California, Santa Barbara, CA 93106 USA.

Digital Object Identifier 10.1109/LPT.2005.851903

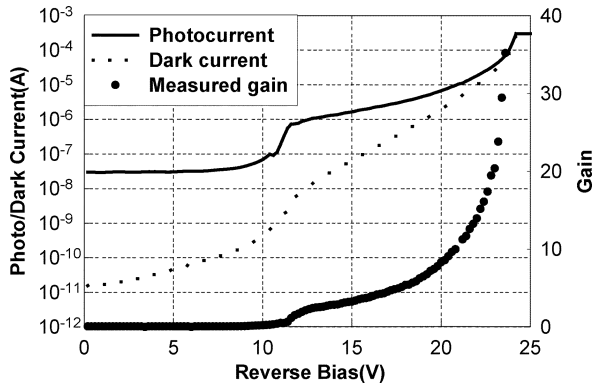


Fig. 2. Current–voltage and gain curves for a 150- μm -mesa-diameter APD.

120-nm-thick $\text{In}_{0.53}\text{Ga}_{0.17}\text{Al}_{0.3}\text{As}$ layer, and an 80-nm-thick $\text{In}_{0.52}\text{Al}_{0.48}\text{As}$ layer with the same P-type doping level. The latter two layers also served as the field control or “charge” region. A 420-nm-thick intrinsic $\text{In}_{0.53}\text{Ga}_{0.47}\text{As}$ layer was grown as the absorbing layer. Undoped InGaAlAs grading layers (50 nm) were inserted to reduce the barrier between $\text{In}_{0.52}\text{Al}_{0.48}\text{As}$ and $\text{In}_{0.53}\text{Ga}_{0.47}\text{As}$ in order to prevent carrier pile-up at the heterointerface. The absorber was slightly p-doped in order to suppress impact ionization in the absorption region [6]. Ideally, the doping in the absorber would be graded to provide a slightly higher field in the direction of the multiplication region. This was approximated by step doping the absorber in two regions, one at $1 \times 10^{16}/\text{cm}^3$ and the other at $4 \times 10^{16}/\text{cm}^3$. After the top grading layer, a 400-nm-thick p-type (Be-doped, $4 \times 10^{18} \text{ cm}^{-3}$) $\text{In}_{0.52}\text{Al}_{0.48}\text{As}$ window layer was grown. The p-type contact layers consisted of 100 nm of $\text{In}_{0.52}\text{Al}_{0.48}\text{As}$ ($\text{Be} : \geq 9 \times 10^{18} \text{ cm}^{-3}$) capped with 50 nm of $\text{In}_{0.53}\text{Ga}_{0.47}\text{As}$ doped at the same level.

The wafers were fabricated into back-illuminated mesa structures using the procedure described in [6].

III. RESULTS AND DISCUSSION

The photocurrent and dark current curves of an 80- μm -diameter APD are shown in Fig. 2. The punch-through voltage was $\sim 12 \text{ V}$ and the breakdown voltage was $\sim 24 \text{ V}$. The photocurrent curve of the APD exhibited a slope after punch-through, an indication of multiplication gain at punch-through. In order to characterize the multiplication gain, the external quantum efficiency (QE) was measured under different bias levels above the punch-through voltage, using a laser operating at $1.55 \mu\text{m}$. At a bias of 15 V, the APD was fully depleted and the measured external QE was $\sim 58\%$. The expected external QE at unity-gain can be estimated by the following expression:

$$\eta_{\text{ext}} = (1 - R) \cdot (1 - e^{-\alpha \cdot d}) \quad (1)$$

where R is the reflection coefficient of the air–semiconductor interface; α is the absorption coefficient of $\text{In}_{0.53}\text{Ga}_{0.47}\text{As}$ at the relevant incident wavelength; and d is the absorption layer thickness. Since the absorption coefficient of $\text{In}_{0.53}\text{Ga}_{0.47}\text{As}$ is $0.705 \mu\text{m}^{-1}$ at $1.55 \mu\text{m}$ [7], for an SACM APD with a 0.42- μm -thick $\text{In}_{0.53}\text{Ga}_{0.47}\text{As}$ absorber, the expected external QE is $\sim 18\%$ assuming an optical transmission of 69% ($R =$

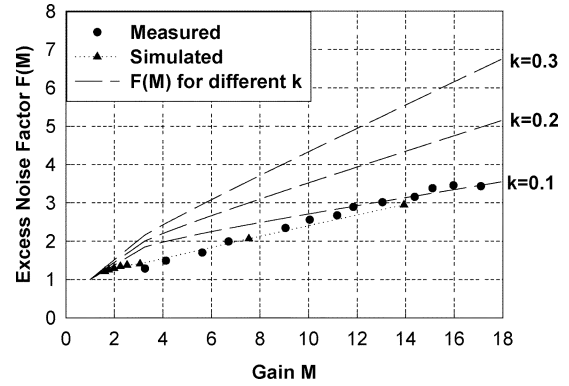


Fig. 3. Simulated and experimental excess noise factor as a function of gain.

0.31) at the air–semiconductor interface (the SiO_2 AR coating was stripped off during the QE measurement in order to reduce uncertainty in the reflectivity). The measured value ($\sim 58\%$) at the reference bias of 15 V is 3.2 times higher than the maximum theoretical value ($\sim 18\%$). We attribute this large QE to the multiplication gain at punch-through, hence the gain at a bias voltage of 15.0 V is estimated to be at least 3.2. The calculated gain curve of an 80- μm -diameter APD is plotted in Fig. 2.

The excess noise factor $F(M)$ was measured following the procedure described in [8]. A semiconductor laser operating at $1.55 \mu\text{m}$ was used as the light source for these measurements. Since there is multiplication gain at punch-through as discussed above, the determination of $F(M)$ is complicated by the fact that the noise value at unity gain, which is the standard reference for this type of measurement, is unknown. This was addressed by using a Monte Carlo simulation to estimate the excess noise factor at $M = 3.2$. The value obtained was $F(M = 3.2) = 1.41$. This then served as the reference point to determine $F(M)$ at higher gains. The measured and simulated $F(M)$ are shown in Fig. 3. The effective k value was estimated to be 0.1 up to a gain of more than 15. We note that this is consistent with noise measurements on PIN-structure $\text{InGaAlAs-InAlAs } I^2E$ APDs [5]. This low noise results from reducing the initial dead space effect for electrons injected from the wide bandgap $\text{In}_{0.52}\text{Al}_{0.48}\text{As}$ into $\text{In}_{0.53}\text{Ga}_{0.17}\text{Al}_{0.3}\text{As}$, which has lower threshold energy [9], [10]. The sloped electric field in the multiplication region also plays an important role in achieving low noise [11]. Electrons are injected from the absorption layer to the multiplication region. They start to impact ionize when the electric field in the charge layer becomes sufficiently high. More and more electron-initiated ionizations occur as the electrons are transported into the multiplication region toward higher electric field. On the other hand, hole impact ionizations in the charge layer are suppressed due to the lower and lower electric field they encounter as they travel back toward the absorber. Hence, there is less reliance on noisy feedback ionization to provide multiplication.

Shown in Fig. 4 is a Monte Carlo simulation of the distribution of impact ionization events in the multiplication region at an average gain of 14. It can be seen that most of the ionization events occur in the $\text{In}_{0.53}\text{Ga}_{0.17}\text{Al}_{0.3}\text{As}$ -well layer. Photon generated electrons drift from the absorption layer toward the charge layer. They gain kinetic energy

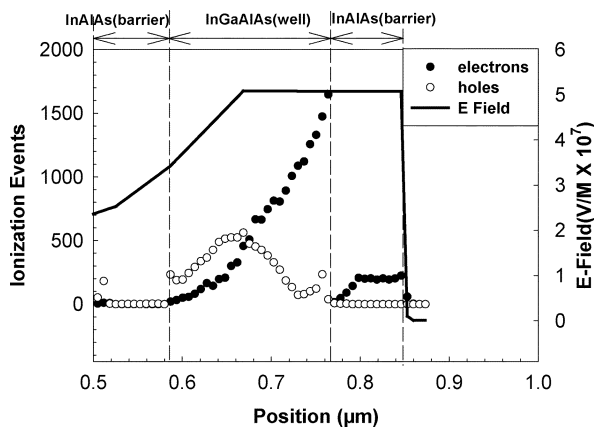


Fig. 4. Simulated impact ionization events distribution and electric field profile as a function of position.

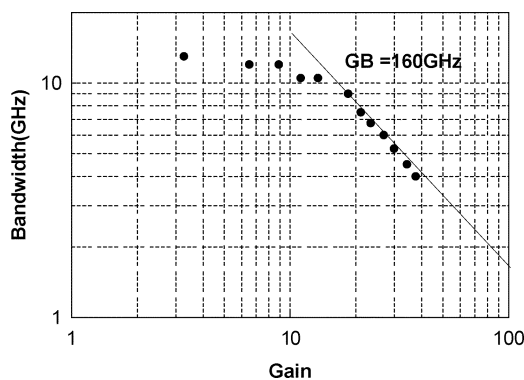


Fig. 5. Measured 3-dB bandwidth versus gain for a 20- μm -mesa-diameter APD.

in the $\text{In}_{0.52}\text{Al}_{0.48}\text{As}$ charge layer where impact ionization events are rare as a result of the large carrier ionization threshold energy in $\text{In}_{0.52}\text{Al}_{0.48}\text{As}$. Once the electrons reach the $\text{In}_{0.53}\text{Ga}_{0.17}\text{Al}_{0.3}\text{As}$ charge layer, where the threshold energy is lower, they ionize quickly. As the electrons travel through the $\text{In}_{0.53}\text{Ga}_{0.17}\text{Al}_{0.3}\text{As}$ charge layer, they encounter higher and higher electric field and initiate more and more impact ionizations. In the undoped $\text{In}_{0.53}\text{Ga}_{0.17}\text{Al}_{0.3}\text{As}$ multiplication layer, the electric field reaches its highest value and the electrons continue to ionize. Once they reach the undoped $\text{In}_{0.52}\text{Al}_{0.48}\text{As}$ layer, although the electric field remains constant, the impact ionization events decrease dramatically due to the higher threshold energy in $\text{In}_{0.52}\text{Al}_{0.48}\text{As}$. Holes generated by electron initiated impact ionization in the $\text{In}_{0.53}\text{Ga}_{0.17}\text{Al}_{0.3}\text{As}$ multiplication region travel in the opposite direction toward the p-contact. However, the hole initiated impact ionization events decrease once holes reach the $\text{In}_{0.53}\text{Ga}_{0.17}\text{Al}_{0.3}\text{As}$ charge layer due to the lower and lower electric field they encounter. This spatial modulation of electron and hole impact ionization events by utilizing the I^2E structure combined with a graded electric field in the multiplication region results in lower excess noise.

S21 RF amplitude measures were made on 20- μm -diameter devices. Fig. 5 shows the 3-dB bandwidth as a function of gain. This device structure is shown to have a gain-bandwidth product

of 160 GHz up to a gain of 40. This gain-bandwidth product is higher than an SACM APD with bulk $\text{In}_{0.52}\text{Al}_{0.48}\text{As}$ multiplication region that has similar multiplication-region-thickness [6]. This is due to the fact that the suppression of hole initiated impact ionization results in reduction of the long tail in the pulse response. The low-gain bandwidth of a typical 20- μm -diameter device is 14 GHz. The calculated resistance–capacitance (RC) limited bandwidth was 15 GHz, which indicates that the bandwidth at low gain was RC limited.

IV. CONCLUSION

We have designed and studied an SACM APD structure that was grown on InP substrate with impact-ionization-engineered multiplication region. Lower noise ($k = 0.1$) and higher speed performance (gain – bandwidth product = 160 GHz) compared to SACM APDs with bulk InAlAs multiplication layer have been achieved.

REFERENCES

- [1] F. Ma, N. Li, and J. C. Campbell, "Monte Carlo simulations of the bandwidth of InAlAs avalanche photodiodes," *IEEE Trans. Electron Devices*, vol. 50, no. 11, pp. 2291–2294, Nov. 2003.
- [2] P. Yuan, S. Wang, X. Sun, X. Zheng, A. L. Holmes Jr., and J. C. Campbell, "Avalanche photodiodes with an impact-ionization-engineered multiplication region," *IEEE Photon. Technol. Lett.*, vol. 12, no. 10, pp. 1370–1372, Oct. 2000.
- [3] S. Wang, F. Ma, X. Li, R. Sidhu, X. G. Zheng, S. Sun, A. L. Holmes Jr., and J. C. Campbell, "Ultra-low noise avalanche photodiodes with a 'centered-well' multiplication region," *IEEE J. Quantum Electron.*, vol. 39, no. 2, pp. 375–378, Feb. 2003.
- [4] F. Ma, S. Wang, X. Li, K. A. Anselm, X.-G. Zheng, A. L. Holmes Jr., and J. C. Campbell, "Monte Carlo simulation of low-noise avalanche photodiodes with heterojunctions," *J. Appl. Phys.*, vol. 92, pp. 4791–4795, Oct. 2002.
- [5] S. Wang, J. B. Hurst, F. Ma, R. Sidhu, X. Sun, X. Zheng, A. L. Holmes Jr., and J. C. Campbell, "Low-noise impact-ionization-engineered avalanche photodiodes grown on InP substrates," *IEEE Photon. Technol. Lett.*, vol. 14, no. 12, pp. 1722–1724, Dec. 2002.
- [6] N. Duan, S. Wang, X. G. Zheng, X. Li, N. Li, J. C. Campbell, C. Wang, and L. A. Coldren, "Detrimental effect of impact ionization in the absorption region on the frequency response and excess noise performance of InGaAs/InAlAs SACM avalanche photodiodes," *IEEE J. Quantum Electron.*, vol. 41, no. 4, pp. 568–572, Apr. 2005.
- [7] X. G. Zheng, J. Hsu, X. Sun, J. B. Hurst, X. Li, S. Wang, A. L. Holmes Jr., J. C. Campbell, A. S. Huntington, and L. A. Coldren, "A 12 \times 12 In Ga As-In Al As avalanche photodiode array," *IEEE J. Quantum Electron.*, vol. 38, no. 11, pp. 1536–1540, Nov. 2002.
- [8] S. Wang, R. Sidhu, X. G. Zheng, X. Li, X. Sun, A. L. Holmes Jr., and J. C. Campbell, "Low-noise avalanche photodiodes with graded impact-ionization-engineered multiplication region," *IEEE Photon. Technol. Lett.*, vol. 13, no. 12, pp. 1346–1348, Dec. 2001.
- [9] O.-H. Kwon, M. M. Hayat, S. Wang, J. C. Campbell, A. Holmes Jr., Y. Pan, B. E. A. Saleh, and M. C. Teich, "Optimal excess noise reduction in thin heterojunction Al_{0.6}Ga_{0.4}As-GaAs avalanche photodiodes," *IEEE J. Quantum Electron.*, vol. 39, no. 10, pp. 1287–1296, Oct. 2003.
- [10] C. Groves, C. K. Chia, R. C. Tozer, J. P. R. David, and G. J. Rees, "Avalanche noise characteristics of single Al_xGa_{1-x}As (0 < x < 0.6)-GaAs heterojunction APDs," *IEEE J. Quantum Electron.*, vol. 41, no. 1, pp. 70–75, Jan. 2005.
- [11] S. A. Plimmer, C. H. Tan, J. P. R. David, R. Grey, K. F. Li, and G. J. Rees, "The effect of an electric-field gradient on avalanche noise," *Appl. Phys. Lett.*, vol. 75, pp. 2963–2965, Nov. 1999.